Rho1 regulates apoptosis via activation of the JNK signaling pathway at the plasma membrane

Amanda L. Neisch,[1,2] Olga Speck,[3] Beth Stronach,[4] and Richard G. Fehon[1,2]

[1]Department of Molecular Genetics and Cell Biology and [2]Committee on Developmental Biology, University of Chicago, Chicago, IL 60637
[3]Department of Pathology and Laboratory Medicine, School of Medicine, University of North Carolina, Chapel Hill, NC 27599
[4]Department of Biological Sciences, University of Pittsburgh, Pittsburgh, PA 15260

Precisely controlled growth and morphogenesis of developing epithelial tissues require coordination of multiple factors, including proliferation, adhesion, cell shape, and apoptosis. RhoA, a small GTPase, is known to control epithelial morphogenesis and integrity through its ability to regulate the cytoskeleton. In this study, we examine a less well-characterized RhoA function in cell survival. We demonstrate that the *Drosophila melanogaster* RhoA, Rho1, promotes apoptosis independently of Rho kinase through its effects on c-Jun NH_2-terminal kinase (JNK) signaling. In addition, Rho1 forms a complex with Slipper (Slpr), an upstream activator of the JNK pathway. Loss of Moesin (Moe), an upstream regulator of Rho1 activity, results in increased levels of Rho1 at the plasma membrane and cortical accumulation of Slpr. Together, these results suggest that Rho1 functions at the cell cortex to regulate JNK activity and implicate Rho1 and Moe in epithelial cell survival.

Introduction

Tissue growth and morphogenesis are often regulated by programmed cell death or apoptosis during development. Although all cells are poised to activate apoptotic mechanisms when triggered by the appropriate extracellular or intrinsic signal, normally, relatively few do so. Thus, cellular mechanisms must exist to restrain apoptosis in the context of normal development. Conversely, loss of the ability to undergo apoptosis is thought to be at the heart of abnormal tissue growth that occurs in many cancers. Previous studies have demonstrated that apoptosis can be induced by activation of the JNK signaling pathway in response to pathogen infection (Takeda et al., 2008), cell competition in imaginal discs (Moreno and Basler, 2004), and morphogen gradient discontinuities (Takatsu et al., 2000; Adachi-Yamada and O'Connor, 2002). In some contexts, JNK is known to be activated downstream of the TNF homologue Eiger (Egr) and its receptor Wengen (Wgn) via a conserved signaling cascade that includes Tak1 (TGF-β–activating kinase 1; a JNK kinase kinase [JNKKK]), Hemipterous (Hep; a JNK kinase), and Basket (Bsk; the sole Jun kinase in *Drosophila melanogaster*; Igaki et al., 2002; Moreno et al., 2002). Downstream of JNK, the core apoptotic machinery, including Hid and caspases, is activated to cause an apoptotic response (Takatsu et al., 2000; Luo et al., 2007).

Although the downstream mechanisms controlling apoptosis are well understood, in many contexts, we understand less about the mechanisms that control activation of the JNK pathway upstream of the apoptotic response. Recent studies suggest that the Rho family GTPases RhoA, Rac, and Cdc42 are important components in JNK signaling during both morphogenesis and apoptosis (for review see Mathew et al., 2009). In epithelial cells, RhoA is known to promote assembly of actin filaments and regulate apical tension via its effectors, including formins and Rho kinase (Rok). Rac and Cdc42 can similarly regulate the cytoskeleton but have more diverse functions such as regulation of epithelial polarity and junctional stability. In addition, Rac is known to regulate apoptosis through activation of the upstream mixed lineage kinases (MLKs). MLKs contain a CRIB (Cdc42 and Rac interactive binding) domain that binds with activated Rac and Cdc42, resulting in kinase activation

Correspondence to Richard G. Fehon: rfehon@uchicago.edu

Abbreviations used in this paper: Bsk, Basket; CA, constitutively active; CRIB, Cdc42 and Rac interactive binding; Dia, Diaphanous; DN, dominant negative; Egr, Eiger; enGal4, engrailed-Gal4; ERM, ezrin/radixin/moesin; GAP, GTPase-activating protein; GDI, GDP dissociation inhibitor; Hep, Hemipterous; IP, immunoprecipitation; JNKKK, JNK kinase kinase; MLK, mixed lineage kinase; Moe, Moesin; POSH, Plenty of SH3s; Puc, Puckered; RHG, *reaper*, *hid*, and *grim*; Rok, Rho kinase; Slpr, Slipper; Wgn, Wengen; Wnd, Wallenda.

The Rockefeller University Press $30.00
J. Cell Biol. Vol. 189 No. 2 311–323
www.jcb.org/cgi/doi/10.1083/jcb.200912010

(Burbelo et al., 1995; Böck et al., 2000). RhoA is also activated in apoptotic cells, although its precise role in the apoptotic process is not well understood (Vidal et al., 2006; for review see Mathew et al., 2009). Interestingly, at least some upstream kinases, including Slipper (Slpr; Polaski et al., 2006), appear to be localized to the plasma membrane. This observation suggests that many of the upstream events in JNK pathway activation occur at the cell cortex, although the functional relevance of this localization has not been elucidated.

The ERM (ezrin/radixin/moesin) proteins function as key organizers of the cell cortex through their ability to interact with the plasma membrane, transmembrane proteins, membrane-associated cytoplasmic proteins, and the underlying cytoskeleton (Bretscher et al., 2002). Recent genetic studies indicate that ERM mutations in a variety of model systems disrupt epithelial integrity, lumen morphogenesis, the apical cytoskeleton, receptor trafficking, and cell survival (Gautreau et al., 1999; Speck et al., 2003; Göbel et al., 2004; Karagiosis and Ready, 2004; Saotome et al., 2004; Chorna-Ornan et al., 2005). Although many of the functions described for ERM proteins involve regulation of the cortical actin cytoskeleton, not all phenotypes seem directly related to this process. For example, in *Drosophila*, the sole ERM protein, Moesin (Moe), has been shown recently to specifically regulate Hedgehog signaling (Molnar and de Celis, 2006). Furthermore, studies indicate that ERM proteins regulate RhoA activity in a variety of cellular contexts (Takahashi et al., 1997; Speck et al., 2003; Molnar and de Celis, 2006).

Of the known ERM functions, perhaps the least well understood is their role in cell survival and apoptosis. A previous study in mammalian cells demonstrated that ectopic expression of a mutation in ezrin Tyr-353, a known substrate for the epidermal growth factor receptor, to a nonphosphorylatable form results in apoptosis (Gautreau et al., 1999). This effect is apparently mediated through the protein kinase Akt, downstream of phosphatidylinositol 3-kinase. Subsequent studies have also implicated ezrin in promoting cell survival, possibly by negatively regulating proapoptotic Fas signaling (Monni et al., 2008; Kuo et al., 2010). However, other studies have suggested that ezrin is proapoptotic in some cells (Parlato et al., 2000; Chakrabandhu et al., 2007). Studies in *Drosophila* have shown that reduction in ERM function results in apoptosis in a Rho1- and JNK-dependent manner (Hipfner and Cohen, 2003; Hipfner et al., 2004; Molnar and de Celis, 2006), although the relationships between these different pathways has not been explored.

The potential connections between epithelial morphogenesis, cell death, and RhoA regulation compelled us to look more closely at the mechanistic basis of apoptosis in *Moe* mutant cells. In this study, we show that Moe negatively regulates cortical levels of Rho1, the *Drosophila* RhoA homologue, in imaginal epithelial cells. In the absence of *Moe* function, JNK signaling is activated in a Rho-dependent fashion, resulting in apoptosis. This effect is dependent on Slpr and Tak1 operating upstream of JNK. Furthermore, we demonstrate that Rho1 binds to Slpr, and unlike Rac and Cdc42, this binding is independent of the Slpr CRIB domain. Intriguingly, Rho1 interacts with Slpr independent of its GTP-binding state and appears to promote Slpr activation via accumulation at the cell cortex. Collectively, these results suggest that Rho1 promotes JNK pathway activity and therefore apoptosis through an interaction with Slpr, an upstream component of the JNK pathway.

Results

Moe mutant cells undergo apoptosis

Our previous work has shown that *Moe*$^{-}$ imaginal disc cells lose epithelial integrity and reside basal to the epithelium (Speck et al., 2003). Further examination showed that many of these cells had pyknotic nuclei, which is reminiscent of cells undergoing apoptosis. In addition, imaginal discs from *Moe*^{G0323} animals were much smaller than those of wild-type animals (Fig. 1, A and B). As noted previously (Molnar and de Celis, 2006), we found that these imaginal discs displayed abundant activated caspase staining (Fig. 1, A and B), indicating apoptotic cells, a phenotype which is suppressed by the expression of a wild-type *Moe* transgene (not depicted). Elevated caspase activity was also observed in cells coexpressing a *Moe* RNAi transgene (Karagiosis and Ready, 2004) and *UAS-GFP* under the control of a *dpp*^{blnk}*-Gal4* driver (*dpp>MoeRNAi*; Fig. 1 D). This effect was cell autonomous, although we noted that some GFP-negative cells were caspase positive (Fig. 1 D″, arrowhead), likely because of the perdurance of *Moe* RNAi as dividing cells move out of the *dpp* expression domain (not depicted). Additionally, we observed cells within the imaginal epithelium that were caspase positive (Fig. S1 A), indicating that apoptosis was not a secondary effect of loss of epithelial integrity.

Moe blocks apoptosis by negatively regulating Rho1 activity

Previous studies have suggested that Moe negatively regulates Rho1 activity in imaginal disc epithelia (Speck et al., 2003; Hipfner et al., 2004; Molnar and de Celis, 2006). If this hypothesis is correct, we would predict that *Moe*$^{-}$ cells should display increased cortical Rho1 because active (GTP bound) Rho1 is primarily associated with the cell membrane. To confirm that this is indeed the case, we used TCA fixation to extract soluble (inactive, GDP bound) Rho, thereby enhancing cortical (active, GTP bound) Rho staining (Yonemura et al., 2004; Piekny et al., 2005). Using *Moe*^{G0323} wing discs that expressed a *UAS-Moe*$^{+}$ transgene in the posterior compartment under the control of an *engrailed-Gal4* (*enGal4*) driver (half-rescued discs), we found that cortical Rho1 staining was increased in *Moe*$^{-}$ cells compared with wild-type cells (Fig. 1 G). Pixel intensities across the boundary between wild-type and mutant cells within the wing epithelium were quantified to confirm this observation (Fig. S2 A). Conversely, overexpression of an activated *Moe* transgene (*Moe*^{T559D}; Speck et al., 2003) reduced levels of apical, cortical Rho1 (Fig. 1 H and Fig. S2 B). These results are consistent with an effect of Moe on localization or stability of Rho1 at the cell cortex, although we cannot exclude the possibility of changes in levels of *Rho1* expression.

Our observation that cortical Rho1 staining is upregulated in *Moe*$^{-}$ epithelial cells suggests that the ability of

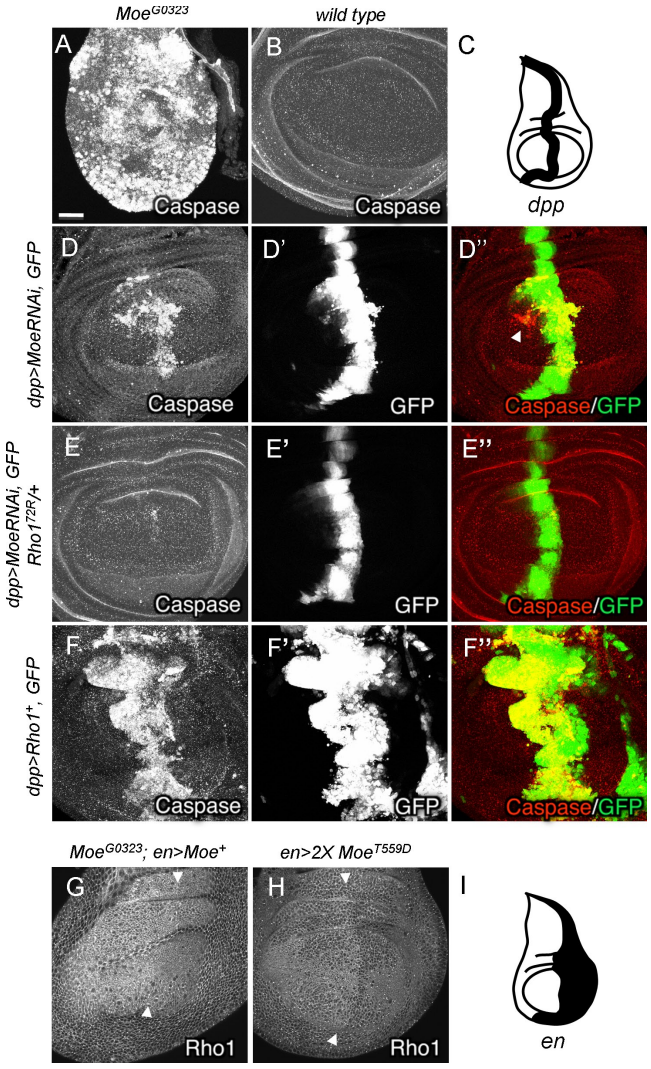

Figure 1. **Moe suppresses apoptosis and the canonical apoptotic cascade.** (A and B) Hemizygous *Moe*^{G0323} wing discs have increased activated caspase staining (A) compared with wild-type wing discs (B). (C) The wing disc expression domain of *dpp-Gal4*, a driver used throughout this study, is illustrated. (D) Expression of a *UAS-Moe* RNAi transgene under a *dpp-Gal4* driver (expression region is marked by *UAS-GFP*; D and D′) also induces apoptosis (merged images shown in D″). Arrowhead in D″ indicates caspase-positive, GFP-negative cells, presumably caused by the perdurance of *Moe* RNAi. Reducing the dosage of *Rho1* (*Rho1*^{72R}/+) in a background expressing the *UAS-Moe* RNAi transgene with the *dpp-Gal4* driver suppresses apoptosis (compare cells in the GFP stripe in E with D). (F) Expression of a *UAS-Rho1*$^{+}$ transgene under the *dpp-Gal4* driver also induces apoptosis. Note that in D′ and F′, the GFP-positive stripe of cells is wider than in wild type because cells that lose epithelial integrity move basally and out of the stripe of *dpp-Gal4* expression. (G) In *Moe*^{G0323} wing cells fixed using TCA, cortical Rho1 protein levels are increased compared with adjacent posterior cells rescued by a *UAS-Moe*$^{+}$ transgene driven by *enGal4* (*en>Moe*$^{+}$). The morphology of this imaginal disc is distorted because of the *Moe* mutation. (H) In contrast, similar expression of two copies of an activated Moe transgene (*en>2X Moe*^{T559D}) results in decreased levels of cortical Rho1 protein. Arrowheads indicate the anterior–posterior compartment boundary, and posterior is to the right in all panels. (I) The wing expression domain of enGal4 is shown. For all genotypes, examples shown are representative of ≥20 imaginal discs examined. Bar, 25 µm.

Moe to promote cell survival might be related to its ability to negatively regulate Rho1. As an initial test, we examined genetic interactions between *Moe* and *Rho1* by expressing the *Moe* RNAi transgene in wing discs heterozygous for a *Rho1*-null mutation. Reducing *Rho1* dosage suppressed apoptosis in *Moe*-depleted cells, suggesting that Rho1 functions together with Moe in apoptosis (Fig. 1 E). This interaction appears specific to the Rho1 GTPase because reducing the dose of *Cdc42* (Fig. S1 O) or all three *Drosophila Rac* orthologues, *Rac1*, *Rac2*, and *Mtl*, simultaneously (Fig. S1 P) did not suppress *Moe* RNAi–induced apoptosis. Furthermore, as shown previously (Vidal et al., 2006), we found that ectopic expression of Rho1 itself induced apoptosis (Fig. 1 F), which is consistent with the model that the apoptotic effects of Moe depletion are caused by increased Rho1 activity.

The apoptotic cascade in *Drosophila* involves induction of one or more of the proapoptotic genes *reaper*, *hid*, and *grim* (RHG). These genes are thought to act by stimulating degradation or suppressing translation of DIAP1, which in turn inhibits activation of the downstream caspases (Holley et al., 2002; Yoo et al., 2002). To determine whether RHG gene expression is up-regulated in *Moe*-deficient and *Rho1*-overexpressing cells, we examined *hid* transcription using a *lacZ* enhancer trap line inserted in the *hid* locus (*hid-lacZ*). We found that *hid* was transcriptionally up-regulated both in *Moe*-deficient cells (Fig. S1 B) and in those overexpressing *Rho1* (Fig. 2, A and B), suggesting that both decreased Moe function and increased Rho1 function induce apoptosis via RHG gene expression.

The JNK pathway regulates apoptosis downstream of Rho1

JNK signaling has been shown to be an important regulator of the apoptotic response in imaginal epithelia (Moreno and Basler, 2004). The JNK pathway is a multilevel kinase cascade that when activated leads to phosphorylation of the transcription factors Jra (Jun-related antigen) and Kay (Kayak), which form the AP1 transcriptional activator complex. To ask whether Rho1-dependent apoptosis involves JNK pathway activity, we determined whether known targets of JNK signaling are up-regulated in Moe-deficient or Rho1-expressing cells. Puckered (Puc), a Jun kinase phosphatase, is a transcriptional target of the JNK signaling pathway and acts in a negative feedback loop to dampen JNK signaling (Martín-Blanco et al., 1998). To examine *puc* activity, we used the *puc*^{E69} allele, which serves as a *lacZ* reporter of *puc* expression and also results in modest up-regulation of JNK signaling. Cells ectopically expressing *Rho1* strongly up-regulated the *puc-lacZ* reporter (Fig. 2, C and D) and underwent apoptosis (Fig. 2, G and H). *Moe*-deficient cells behaved similarly (Fig. S1, C–H). We also observed increased expression of Mmp1 (Matrix metalloproteinase 1) in Rho1-overexpressing cells (Fig. 2, E and F), which is an independent readout for JNK activity (Uhlirova and Bohmann, 2006), supporting the notion that JNK signaling is activated by increased levels of Rho1.

To ask whether JNK pathway activity is involved in *Rho1*-induced apoptosis, we conducted genetic interaction experiments by reducing the dosage of different components of the JNK pathway in tissues expressing a *UAS-Moe* RNAi or *UAS-Rho1*$^{+}$ transgene. Initially the genetic interaction experiments were conducted in tissues expressing the *UAS-Moe*

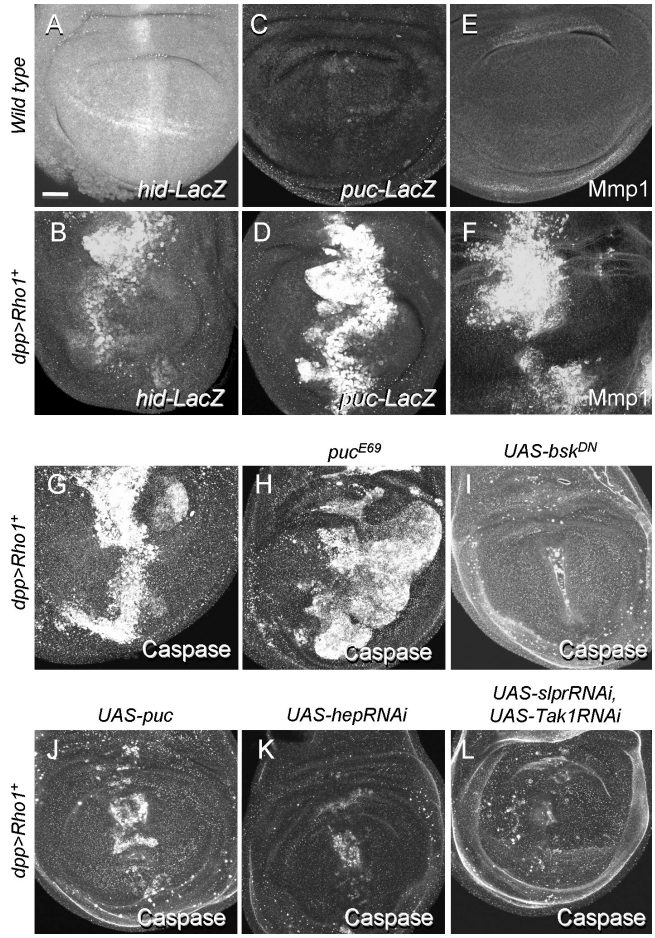

Figure 2. **Ectopic Rho1 expression induces JNK pathway activation and apoptosis.** (A and B) Compared with wild-type discs (A), a reporter for *hid*, a proapoptotic gene and canonical apoptotic pathway component, is strongly up-regulated in cells that express a *UAS-Rho1*$^{+}$ transgene (B). (C and D) *puc-lacZ*, a reporter for JNK signaling, is increased in *dpp-Gal4; UAS-Rho1*$^{+}$–expressing cells. (E and F) Mmp1, an additional downstream target of JNK signaling, is also up-regulated in cells expressing the *Rho1* transgene (compare E with F). (G and H) Apoptosis, caused by expression of *dpp-Gal4; UAS-Rho1*$^{+}$ (*dpp>Rho1*; G) is increased by reducing the dosage of *puc* (H) and thereby increasing JNK signaling. (I–K) Conversely, apoptosis induced by *dpp>Rho1*$^{+}$ is suppressed by blocking JNK signaling at the level of Bsk (*UAS-bsk*^{DN} [I] or *UAS-puc* [J]), the sole Jun kinase, or Hep (*UAS-hepRNAi*; K), a JNK kinase. (L) Knockdown of both Slpr and Tak1, two JNKKKs, together in *dpp>Rho1*$^{+}$-expressing cells suppresses apoptosis to a large extent. For all genotypes, examples shown are representative of ≥20 imaginal discs examined. Bar, 25 µm.

RNAi transgene because a recombinant chromosome of *dpp-Gal4*^{blnk}, *UAS-Moe* RNAi can be maintained as a viable stock (making the genetics simpler), whereas *dpp-Gal4*^{blnk}, *UAS-Rho1*$^{+}$ cannot be maintained as a stock because of higher levels of Rho1 expression. Each positive genetic interaction found in the *Moe* RNAi background was confirmed in the *UAS-Rho1*$^{+}$ background. We first examined Bsk, the sole Jun kinase in *Drosophila*. We found that reducing Bsk levels, using a *bsk*^{DN} transgene, suppressed apoptosis in Rho1-expressing cells (Fig. 2 I). Similarly, overexpression of Puc, which negatively regulates Bsk, strongly suppressed apoptosis in Rho1-expressing cells (Fig. 2 J). Similar results were observed in cells lacking *Moe* function using either a *bsk* RNAi (Fig. S1 I) or *bsk*^{DN} transgene (not depicted) as well as by overexpressing Puc (Fig. S1 J). These results suggest that Bsk functions together with Rho1 in regulating apoptosis.

To further define how JNK signaling is activated, we looked at upstream JNK pathway components. Two proteins, Hep and Mkk4 (Map kinase kinase 4), function at the level of JNK kinase in *Drosophila*. Hep is involved in dorsal closure, cell shape changes, and epithelial morphogenesis (Glise et al., 1995; Agnès et al., 1999). In contrast, little is known about how Mkk4 functions. Expression of a *hep* RNAi transgene suppressed Rho1-induced apoptosis (Fig. 2 K). A similar suppression was seen with the *hep* RNAi transgene and the *hep*^{R75} hypomorphic allele in Moe-deficient cells (Fig. S1 L, and not depicted). In contrast, reducing the levels of Mkk4 in Moe-deficient cells by RNAi or an insertional mutation had no effect on apoptosis (unpublished data).

Upstream of Hep in the JNK pathway are five *Drosophila* JNKKKs: Mekk1, Tak1, Slpr, Ask1 (Apoptotic signal-regulating kinase 1), and Wallenda (Wnd). JNK signaling is activated for diverse cellular processes, and the JNKKK level of the pathway is thought to be where specificity is achieved. Mekk1 is activated in stress response (Ryabinina et al., 2006), Slpr is required for dorsal closure and morphogenesis (Stronach and Perrimon, 2002; Polaski et al., 2006), Wnd regulates synaptic growth (Collins et al., 2006), Tak1 is involved in innate immunity and apoptosis (Takatsu et al., 2000; Igaki et al., 2002; Park et al., 2004; Geuking et al., 2005), and Ask1 is involved in apoptosis (Kuranaga et al., 2002; Ryabinina et al., 2006). All five JNKKKs are transcribed in wing discs (unpublished data). However, knockdown of any of these kinases singly using RNAi or dominant-negative (DN) transgenes has no visible effect on apoptosis in Moe-deficient wing discs (unpublished data), raising the possibility of functional redundancy at the JNKKK level. We note that with the exception of the *wnd* RNAi line, all of these JNKKK RNAi or DN lines have been tested for efficacy by us (*UAS-slpr* RNAi; unpublished data) or by others (*Mekk1* RNAi [Brun et al., 2006], *Tak1* DN [Takatsu et al., 2000], *Tak1* RNAi [Igaki et al., 2006], and *Ask1* DN [Kuranaga et al., 2002; Kuranaga and Miura, 2005]).

To examine the possibility of functional redundancy between JNKKKs, we first depleted Tak1 and Ask1 in *Moe* mutant cells because both have been shown to be involved in apoptosis, but found no effect (unpublished data). Recently, Polaski et al. (2006) reported that reducing the level of Tak1 in *slpr* mutants increases the percentage of embryos with dorsal closure defects, suggesting partial functional redundancy between these genes. Additionally, they found that *slpr*-null mutants have misoriented male genitalia, which is a phenotype observed in animals with apoptotic defects (Macías et al., 2004; McEwen and Peifer, 2005; Polaski et al., 2006). To ask whether Slpr and Tak1 might function redundantly, we depleted both by RNAi in Rho1-expressing cells. We found that this treatment significantly suppressed apoptosis (Fig. 2 L), as it did in Moe-depleted cells (Fig. S1 M), which is consistent with the idea that Slpr and Tak1 function downstream of Rho1.

Further upstream of the JNK pathway in some tissues are the TNF ligand Egr and its receptor Wgn. Transcripts from both

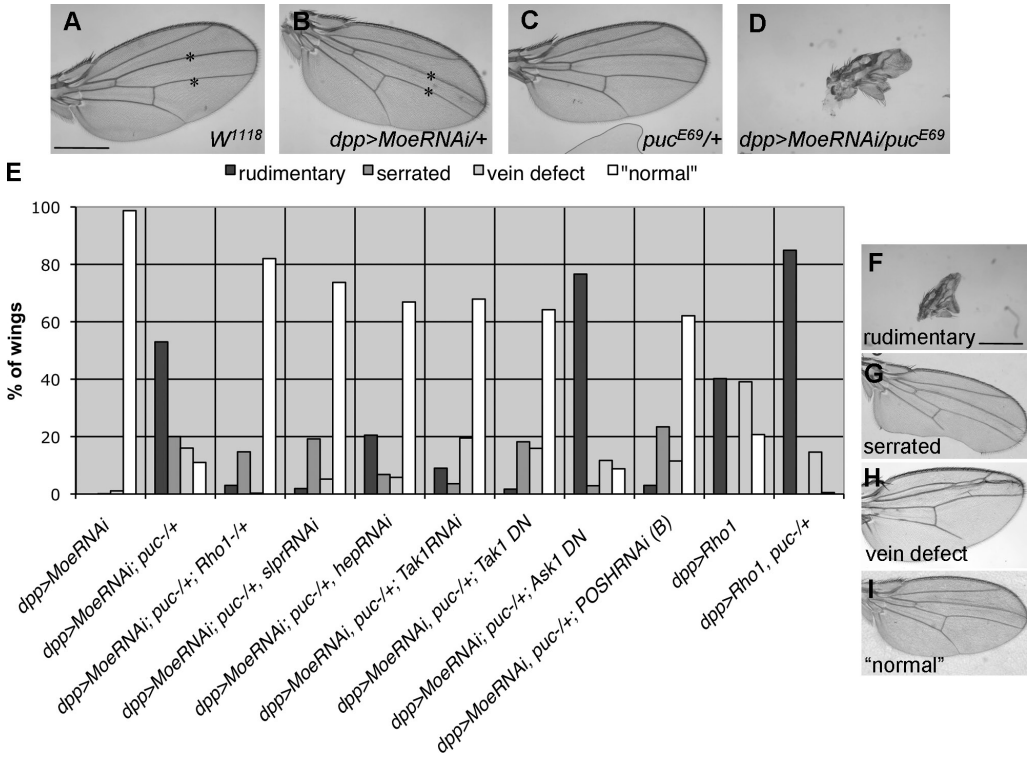

Figure 3. **Hep, Tak1, and Slpr function together with Moe and Rho1 in the adult wing.** (A and B) Expression of *dpp>MoeRNAi* on its own slightly reduces the area in the region of expression between wing veins L3 and L4 (marked by asterisks; compare A with B) but does not otherwise affect wing morphology. (C) Reducing *puc* dosage alone has no phenotype. However, reducing *puc* dosage in the *dpp>MoeRNAi* background or in a *dpp>Rho1* background severely reduces the wing blade (quantifications in E; example of phenotype in *dpp>MoeRNAi* background in D). (E) This phenotype is suppressed by reducing the level of *Rho1*, *slpr*, *hep*, *Tak1*, or *POSH* but not by reducing the activity of *Ask1*. For quantification, $n > 400$ wings for each genotype. (F–I) Wing phenotypes scored were rudimentary (F), serrated (G), vein defect (H), and normal (I), which has a reduction in the area between wing veins L3 and L4. Bars, 475 µm.

of these genes are present in wing discs (unpublished data). However, knockdown of either *egr* or *wgn* had no visible effect on apoptosis in *Moe* mutant cells (unpublished data), suggesting that Rho1 interacts with JNK signaling independently of these components.

The data presented so far support a model in which elevated Rho1 activity in Moe^{-} cells results in activation of JNK signaling and induction of apoptosis. To provide a quantitative assay for interactions between *Moe*, *Rho1*, and members of the JNK pathway, we examined phenotypic interactions between these genes in the adult wing. Wings from *dpp>MoeRNAi* adults had a reduced area between veins 3 and 4, where the *Gal4* driver is expressed (Fig. 3, compare A with B). Although reducing the dosage of *puc* alone had no wing phenotype (Fig. 3 C), when combined with *dpp>MoeRNAi*, it caused a severely reduced or rudimentary wing phenotype (Fig. 3, D and E). An identical phenotype was seen when *dpp>Rho1* was expressed in combination with reducing *puc* dosage (Fig. 3 E). Similar phenotypes have been described for *dpp* regulatory alleles (Masucci et al., 1990; Bangi and Wharton, 2006), suggesting that the rudimentary wing phenotype is caused by apoptosis-induced ablation of the Dpp-expressing cells, resulting in severe disruption of the Dpp-patterning gradient.

In light of these results, we reasoned that the adult wing phenotype of *dpp>MoeRNAi*, puc^{E69}/+ animals might provide a highly sensitive background in which to study the effects of pathway components involved with Moe in regulating apoptosis. Consistent with this idea, we found that removing one copy of *Rho1* strongly suppressed the *dpp>MoeRNAi*, puc^{E69}/+ phenotype (Fig. 3 E). Similarly, reducing Hep, Slpr, or Tak1 activity suppressed this phenotype, which is consistent with our results in imaginal discs (Fig. 2, K and L). In contrast, reducing the level of Ask1 had no effect (Fig. 3 E), and Wnd and Mekk1 knockdown gave an intermediate result (not depicted), suggesting that either these JNK pathway components are not involved downstream of Rho1 or that these transgenes do not reduce gene function efficiently enough to observe an effect.

Rho1 forms a complex with Slpr

To address how Rho1 regulates JNK activity upstream of apoptosis, we first looked at downstream effectors of Rho1. We examined a possible role for the two major Rho1 effectors, Diaphanous (Dia) and Rok. Expression of a constitutively active (CA) *dia* transgene results in apoptosis (Janody and Treisman, 2006), but expression of a *dia* RNAi transgene did not affect apoptosis in Moe-deficient cells (Fig. S3 B), even though it did strongly reduce Dia protein (Fig. S3 C). Similarly, expression of a previously characterized CA *rok* transgene (rok^{CA}; Winter et al., 2001) failed to induce apoptosis (Fig. S3 D). The effectiveness of this transgene was confirmed because it caused the formation of a furrow in the expressing cells similar to that formed by the expression of UAS-$Rho1^{+}$ (Fig. 2 I). The phenotypic

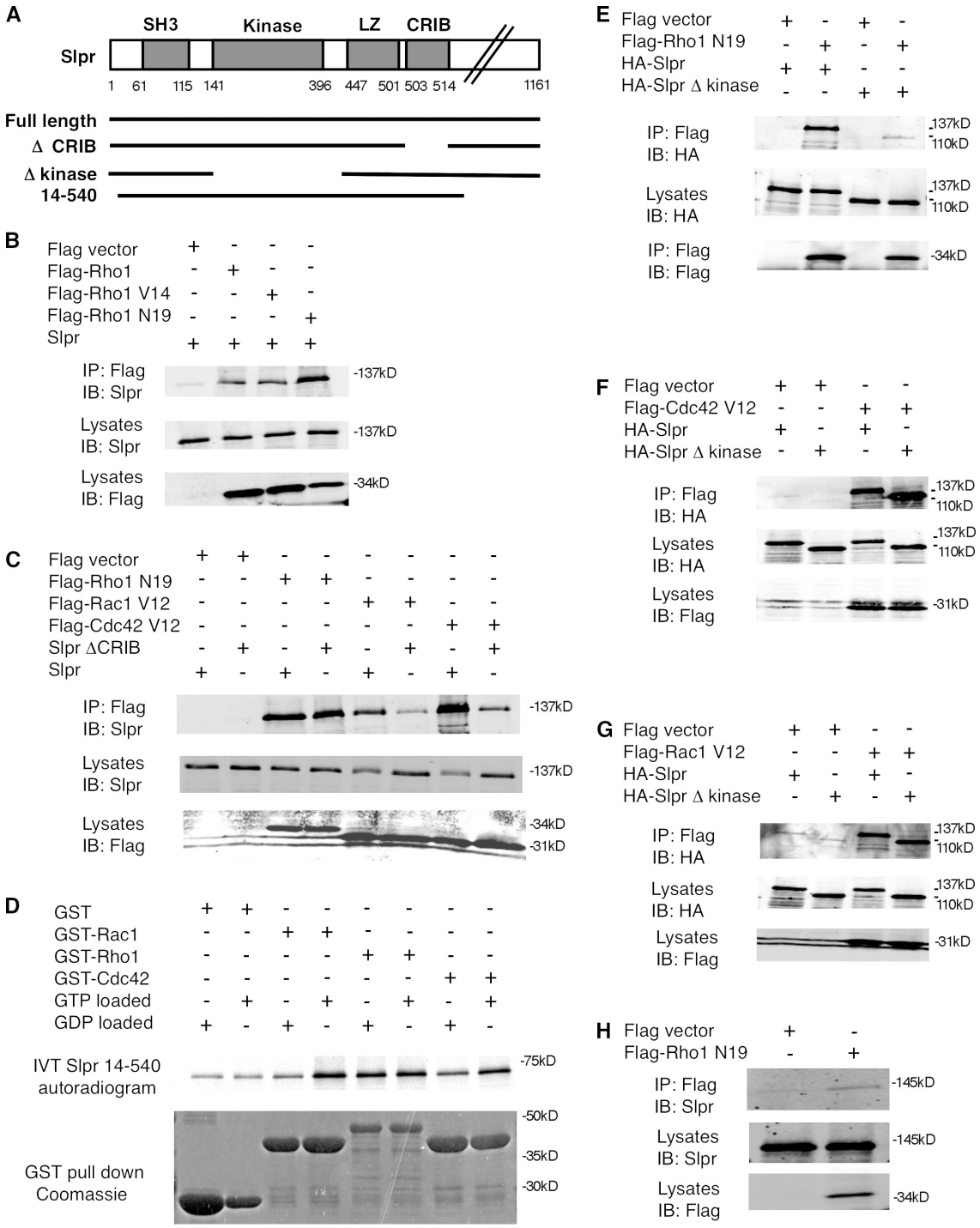

Figure 4. **Rho1 interacts with Slpr independent of its GTP-binding state.** (A) A schematic diagram of the structure of the Slpr indicating different domains and their amino acids coordinates. Lines below indicate constructs used to determine regions required for interactions with Rho1. LZ, Leu zipper domain. (B and C) S2 cells were cotransfected with expression constructs for the indicated forms of Slpr, Rho1, Cdc42, and Rac1. (B) Wild-type, CA ($Rho1^{V14}$), and DN ($Rho1^{N19}$) forms of Rho1 all coimmunoprecipitate with full-length Slpr protein, although $Rho1^{N19}$ is consistently the strongest. (C) Deletion of the CRIB domain greatly diminishes interaction between Slpr and the CA forms of Cdc42 ($Cdc42^{V12}$) and Rac1 ($Rac1^{V12}$) but does not affect interaction with Rho1. (D) In vitro–translated Slpr containing the SH3, kinase, Leu zipper, and CRIB domains preferentially binds to GTP-loaded Rac1 and Cdc42-GST fusion proteins. In contrast, this domain shows no preference for GTP- versus GDP-loaded Rho1. (E–G) The kinase domain of Slpr is required for co-IP with Rho1 (E) but not for co-IP with Cdc42 (F) or Rac1 (G). (H) Endogenous Slpr from cultured S2 cells coimmunoprecipitates with DN Rho1 ($Rho1^{N19}$). IB, immunoblot.

difference between ectopic Rho1 and Rok^{CA} expression suggests that increased actin–myosin contractility alone is not sufficient to cause apoptosis and that Rho1-mediated apoptosis does not involve either Dia or Rok.

As an alternative model, we considered the possibility that Rho1 activates JNK signaling through binding to an upstream component of the pathway. Previous studies have shown that the Rho family GTPases Cdc42 and Rac1 bind to and activate

the MLK subfamily of Ser/Thr kinases (for review see Gallo and Johnson, 2002). Activation of MLKs occurs by binding of the GTPase to the CRIB domain, which is thought to relieve autoinhibition of the protein for kinase activation (Burbelo et al., 1995; Böck et al., 2000). Although Rho itself has not been previously implicated in this role, we wondered whether Rho1 might bind to the *Drosophila* MLK homologue, Slpr, thereby activating JNK signaling. In accordance with previous studies (Teramoto et al., 1996; Böck et al., 2000), we found that in *Drosophila* cultured cells, Slpr preferentially coimmunoprecipitated with the constitutively GTP-bound form of Cdc42 ($Cdc42^{V12}$). Preference for the CA ($Rac1^{V12}$) versus DN forms ($Rac1^{N17}$) of Rac1 was less obvious but still apparent (unpublished data). We also found that Rho1 coimmunoprecipitated with Slpr, but to our surprise, the DN, GDP-bound form of Rho1 ($Rho1^{N19}$) coimmunoprecipitated most strongly (Fig. 4, A and B). Reciprocal coimmunoprecipitations (co-IPs) gave similar results (not depicted), and we observed that endogenously expressed Slpr protein in cultured cells coimmunoprecipitated with $Rho1^{N19}$ (Fig. 4 H). Consistent with the observation that $Rho1^{N19}$ forms a complex with Slpr, expression of the *UAS-Rho1*^{N19} transgene in wing discs induced apoptosis through JNK signaling (Fig. 5, A and B).

Because activated Cdc42 and Rac1 are thought to directly bind to MLKs through an interaction with the CRIB domain, we assessed whether the co-IP of Rho1 with Slpr is also dependent on this domain. We compared the ability of activated Cdc42 and Rac1 or DN Rho1 to coimmunoprecipitate with a form of Slpr from which the CRIB domain was deleted ($Slpr^{\Delta CRIB}$). As expected, $Slpr^{\Delta CRIB}$ coimmunoprecipitated only weakly with Cdc42 and Rac1 (Fig. 4 C). Surprisingly, co-IPs between the DN form of Rho1 and Slpr were unaffected by the CRIB deletion, demonstrating that the ability of Rho1 to form a complex with Slpr is independent of the CRIB domain (Fig. 4 C).

To map more precisely the domain required for interaction with Rho1, we constructed domain-specific Slpr deletions. We found that an N-terminal construct ($Slpr^{1–432}$), which contains just the SH3 and kinase domains, coimmunoprecipitated with Rho1, as did a construct with only the SH3 domain deleted (unpublished data). In contrast, deletion of the kinase domain ($Slpr^{\Delta kinase}$) greatly diminished the formation of a Slpr–Rho1 complex but did not noticeably alter the co-IP of Cdc42 or Rac1 (Fig. 4, E–G). These results suggest that the kinase domain is specifically required for Rho1–Slpr interactions but not for interactions between Slpr and either Rac or Cdc42. Experiments designed to test whether the kinase domain is sufficient for Rho1–Slpr co-IP gave ambiguous results because the Slpr kinase domain appeared to interact nonspecifically with all Rho family GTPases when expressed on its own (unpublished data).

Because Rho1 has not been reported previously to bind to MLKs, we wished to confirm the interaction using in vitro pull-down assays. An in vitro–translated N-terminal Slpr construct ($Slpr^{14–540}$) containing the SH3, kinase, and CRIB domains bound to GST-Rho1 (Fig. 4 D), suggesting that the two proteins interact directly. Consistent with our co-IP experiments using S2 cells, in vitro pull-down assays showed that GTP-bound Rac1

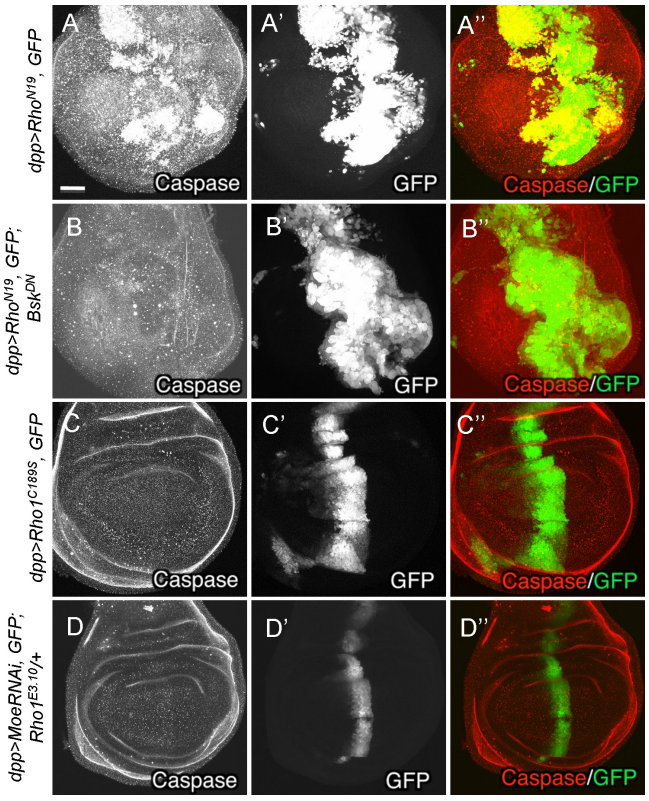

Figure 5. **Rho1-induced apoptosis is dependent on its cortical localization.** (A) Expression of a DN *Rho1* (*Rho1*^{N19}) transgene under the *dpp-Gal4* driver induces apoptosis. (B) This effect requires JNK signaling, as inhibiting Bsk by expressing a DN transgene in cells expressing $Rho1^{N19}$ suppresses apoptosis. (C) Expression of a Rho1 transgene with a missense mutation (C189S) in the CAAX box does not result in apoptosis. (D) Reducing the level of cortically localized Rho1 using an allele of *Rho1* (*Rho1*$^{E3.10}$) with a missense mutation (C189Y) in the CAAX box suppresses apoptosis caused by expression of the *UAS-Moe* RNAi transgene under *dpp*^{blk}*-Gal4* (*dpp>MoeRNAi*). Bar, 25 µm.

and Cdc42 bound to Slpr preferentially, whereas Rho1 bound to Slpr regardless of its GDP/GTP-binding state (Fig. 4 D). Although these data strongly suggest that Slpr and Rho1 interact directly, we note the possibility that other proteins necessary for complex formation may be present in the in vitro translation mixture.

Because both Slpr and Tak1 act redundantly in apoptosis in Rho1-expressing cells in the wing disc, we asked whether Tak1 is also in a complex with Rho1 or Slpr. We found that Tak1 coimmunoprecipitated with both Slpr and Rho1 in cultured cells (Fig. S4 A), which is consistent with the possibility that a larger protein complex may form for activation of the JNK pathway, although we have not yet tested this directly.

Rho1 regulates Slpr subcellular localization

Our results suggest that Rho1 binding to Slpr activates JNK signaling and that in this context, the nucleotide-binding state of Rho1 is unimportant. Because both Rho1 and Slpr localize cortically in cells, we wondered whether Rho1 subcellular localization is important for JNK activation. If cortically localized Rho1 promotes JNK pathway activation, a mutation that disrupts Rho1 localization should be incapable of activating JNK signaling. To test this idea, we generated a *UAS-Rho1*^{C189S}

transgene, which encodes Rho1 with a mutation in the CAAX box, which is the site of posttranslational lipid modification required for membrane association. Expression of this transgene, at similar or greater levels than the *UAS-Rho1*$^{+}$ and *UAS-Rho1*^{N19} transgenes (Fig. S5, A–D), did not induce apoptosis (Fig. 5 C). Importantly, Rho1^{C189S} coimmunoprecipitated with Slpr to a similar extent as the other Rho1 alleles (Fig. S5 E), suggesting that forming a complex with Rho1 alone is not sufficient to activate Slpr and instead that localization at the plasma membrane is important. In addition, we asked whether heterozygosity for the *Rho1*$^{E3.10}$ allele, which carries a missense mutation (C189Y) in the CAAX box (Halsell et al., 2000), therefore reducing the level of membrane-bound Rho1 by half (while leaving the total Rho1 levels unchanged), behaves similarly to other *Rho1* alleles in suppressing *Moe* phenotypes. This mutation suppressed apoptosis in *Moe*$^{-}$ cells as effectively as the null *Rho1* allele (Fig. 5 D compared with Fig. 1 [D and E]), again suggesting that Rho1 subcellular localization, not the overall protein level of Rho1, is important for activation of the JNK signaling pathway.

If Rho1 at the cell cortex interacts with Slpr to promote its activation, we predict that cells with increased cortical Rho1 should display increased Slpr levels. To test this, we examined Slpr localization and abundance in *Moe* mutant cells, which we have demonstrated display increased levels of cortical Rho1 (Fig. 1 G). As predicted, anti-Slpr staining was up-regulated in wing imaginal disc cells depleted of Moe function with an RNAi transgene (Fig. 6, A and B). To examine this further, we quantified Slpr staining pixel intensity in this epithelium comparing sections through the apical domain with more basolateral sections for four discs, all of which gave similar results. Rho1 staining is primarily localized to the apical domain; thus, we expect that if the observed Slpr abundance is Rho1 dependent, Slpr should be increased primarily in the apical domain. Antibody staining revealed that Slpr protein level was increased specifically in the apical domain of *Moe*$^{-}$ cells compared with wild-type cells (Fig. 6 C) but did not change basally, as predicted.

Scaffolding proteins that link together multiple signaling components are known to play an important role in the JNK pathway (Dhanasekaran et al., 2007). POSH (plenty of SH3s) is a scaffolding protein that mediates JNK activation during apoptosis in mammalian fibroblasts (Tapon et al., 1998), neurons (Xu et al., 2003), and *Xenopus laevis* embryos (Kim et al., 2005). In vertebrate systems, POSH is known to interact with MLK (JNKKK) family members, JNK kinases, and JNKs (Xu et al., 2003). To ask whether *Drosophila* POSH functions in JNK pathway activation in Moe-deficient cells, we depleted POSH by transgenic RNAi in *Moe*$^{-}$ imaginal disc cells and found dramatically decreased apoptosis (Fig. S1 N). Knockdown of POSH also suppressed the adult wing phenotype of *dpp>MoeRNAi*, *puc*^{E69}/+ animals (Fig. 3 E). We found that POSH coimmunoprecipitated with Rho1, Slpr, and Tak1 (Fig. S4 B), suggesting that these proteins form a complex when expressed in S2 cells. Collectively, our results suggest a model in which cortically localized Rho1, whose levels are negatively regulated by Moe, promotes the formation of a complex consisting of Slpr, POSH, and other upstream components of the JNK pathway, resulting in pathway activation (Fig. 7).

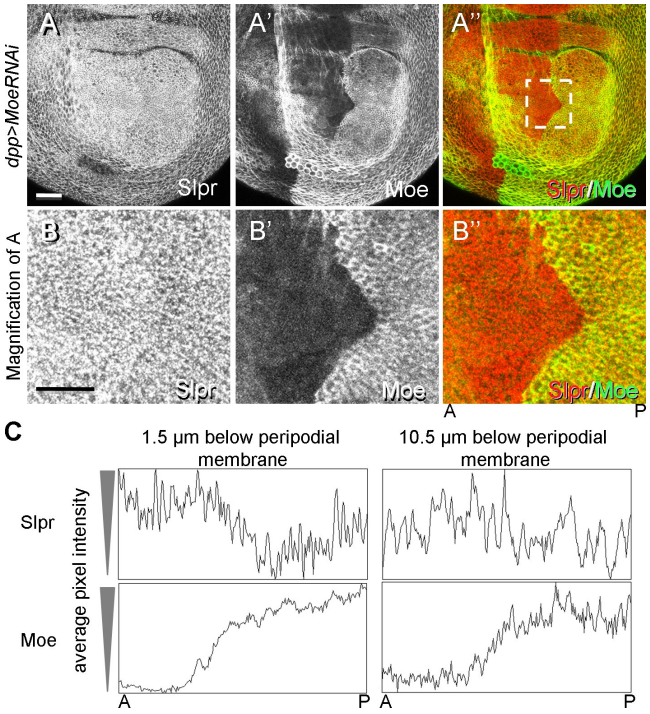

Figure 6. **The cortical abundance of Slpr is increased in *Moe* mutant cells.** (A) Expression of *dpp>MoeRNAi* results in increased apical Slpr localization. (B) A higher magnification view of the region indicated by the box in A″ is presented showing increased Slpr punctate localization in the apical domain of *Moe*-depleted cells. (C) Pixel intensity across the region of the disc, from anterior (A) to posterior (P), shown in B indicates that when Moe levels are knocked down, apical (1.5 µm below surface) Slpr levels are much greater than in the wild-type cells. More basally (10.5 µm below surface), Slpr levels are uniform. Bars, 25 µm.

Discussion

Studies in *Drosophila* have suggested that Rho GTPases operate upstream of the JNK pathway activation in morphogenesis and that JNK activation in epithelial cells results in apoptosis (Igaki et al., 2002; Kuranaga et al., 2002; Moreno et al., 2002; Stronach and Perrimon, 2002; Woolner et al., 2005). However, to date, there has been only a single report of a role for Rho1 in apoptosis in *Drosophila* (Vidal et al., 2006), and the mechanistic basis for this role has not been explored. Based on observations that Moe-deficient cells undergo apoptosis and display increased Rho1 activity (Fig. 1; Hipfner and Cohen, 2003; Speck et al., 2003; Hipfner et al., 2004; Molnar and de Celis, 2006), we have investigated a possible role for Rho1 in apoptosis in the imaginal disc epithelium. We have demonstrated that increased Rho1 at the cell cortex, caused either by loss of *Moe* function or ectopic *Rho1* expression, triggers apoptosis via JNK pathway activation. Based on our results, we propose a model in which membrane-associated Rho1 forms a complex with Slpr, an MLK which functions upstream of JNK, thereby activating Slpr and downstream components of the JNK pathway at the cell cortex and inducing apoptosis (Fig. 7). These results strongly implicate Moe and Rho1 as potential upstream

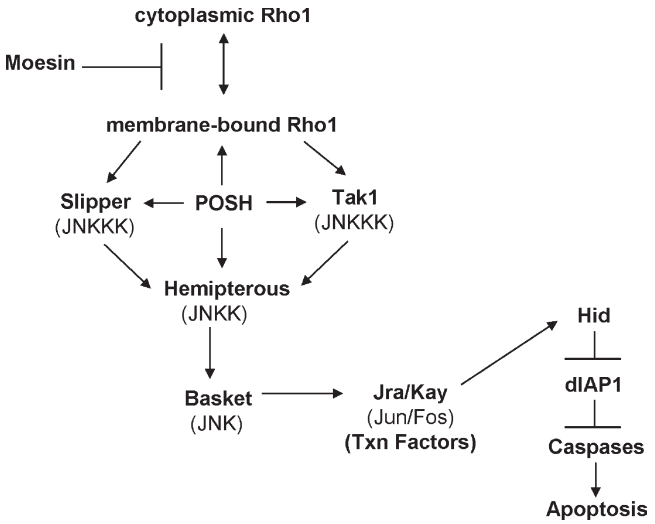

Figure 7. **A model for Moe and Rho1 function in apoptosis based on genetic, biochemical, and subcellular localization data.** Moe negatively regulates Rho1 activity, at least in part by preventing its localization to the cell cortex. Cortical Rho1 forms a complex that contains Slpr, Tak1, Hep, and POSH and functions to activate the JNK pathway. Downstream of the JNK pathway, *hid* transcription is up-regulated to trigger apoptosis.

regulators of JNK signaling in developing epithelial cells, upstream of apoptosis.

Consistent with our model that membrane-associated Rho1 promotes the formation of a Slpr-containing complex at the cell cortex, a recent study showed that endogenous Slpr is cortically localized in epithelial cells (Polaski et al., 2006). Furthermore, we have shown that loss of Moe and a concomitant increase in cortical Rho1 results in increased Slpr accumulation at the cell cortex (Fig. 6). In addition to interacting with Slpr, we found that Rho1 coimmunoprecipitates with both Tak1 (Fig. S4 A) and Hep (not depicted), which is consistent with our genetic interaction data in imaginal discs and adult wings (Fig. 2, K and L; and Fig. 3 E). MLKs such as Slpr are known to interact with scaffolding proteins that link together multiple kinase components in the pathway. We have found that reducing POSH, a JNK scaffolding protein, can suppress loss of *Moe*-induced apoptosis (Fig. 3 E and Fig. S1 N) and that POSH can form a complex with Rho1, Slpr, and Tak1 in cultured *Drosophila* cells (Fig. S4 B). These results are consistent with a model in which Rho1 and Slpr form a complex together with other JNK components to activate the JNK pathway, although we have not demonstrated that all four components are present in a single complex.

An alternative model for the induction of apoptosis in Moe-deficient and Rho1-overexpressing cells is that cytoskeletal disruption and loss of epithelial integrity, which are characteristic of these manipulations, trigger the apoptotic response. For example, a process termed anoikis has been described in mammalian epithelia in which cells that lose contact with the basal lamina undergo apoptosis via mechanisms that are not well understood (Ma et al., 2007). However, the evidence suggests that anoikis or a similar mechanism is not at work in Moe-deficient cells in the following ways. Blocking activation of matrix metalloproteinases in Moe-deficient cells, and thereby preventing basal lamina breakdown, does not prevent cell death (unpublished data). Similarly, blocking apoptosis in Moe-deficient cells does not prevent the loss of epithelial integrity and extrusion from the epithelium. In addition, we observed activated caspase staining in Moe^{-} cells that were still well integrated into the imaginal epithelium (Fig. S1 A), suggesting that loss of cell or basal lamina contact is not required for the induction of the apoptotic response.

Several important questions regarding our model for Moe's requirement for cell survival remain unanswered. Although Moe is known to regulate Rho1 activity, we do not yet understand the mechanistic basis of this functional interaction. Previous studies have described interactions between ERM proteins and Rho guanine nucleotide exchange factors (Takahashi et al., 1998; D'Angelo et al., 2007), a Rho GTPase-activating protein (GAP; Hatzoglou et al., 2007), and Rho GDP dissociation inhibitor (GDI; Takahashi et al., 1997), although their functional significance in vivo has not been examined. In principle, any of these interactions could explain the effects of *Moe* loss of function on Rho1 activity, including the apparent alteration in Rho1 cortical abundance in Moe^{-} tissues. For example, if Moe inhibits the activity of a Rho guanine nucleotide exchange factor at the cell cortex, cells lacking Moe function would be expected to accumulate cortical Rho1. Conversely, if Moe positively regulates a Rho GAP, perhaps by interacting with and recruiting the GAP to the cortex, a similar phenotype is expected in Moe-deficient cells.

A particularly intriguing aspect of the results presented in this study is the observation that Rho1 binding to Slpr and activation of the JNK pathway are independent of GTP binding (Fig. 4, B and D; and Fig. 5, A and B). Although GTP-independent activation of JNK signaling by Rho1 seems surprising, we note that this finding is consistent with previous observations that expression of DN $Rho1^{N19}$ is sufficient to activate the JNK pathway (Bloor and Kiehart, 2002) and that expression of wild-type Rho1 induces apoptosis in imaginal epithelia (Vidal et al., 2006). Together with our observation that cortical Rho1 staining is enhanced in Moe-deficient cells and decreased in cells that express an activated *Moe* transgene, these results suggest that the ability of Rho1 to control JNK pathway activity may be mediated by its subcellular localization rather than its GTP-binding state. However, it is important to note that in most contexts, these two aspects of Rho1 function are tightly linked. Normally, only GTP-bound Rho is localized to the cell cortex because Rho GDP is bound to Rho GDI in the cytoplasm (for review see Dovas and Couchman, 2005). However, in situations in which Rho1 is ectopically expressed at higher than normal levels, endogenous Rho GDI may be titrated out, allowing Rho1 to associate with the plasma membrane regardless of its activation state. Consistent with this idea, we found that when expressed at high levels, $Rho1^{N19}$ is cortically localized (not depicted) and triggers activation of JNK signaling and apoptosis as effectively as does wild-type Rho1 (Fig. 5 A). In contrast, $Rho1^{C189S}$, a form of Rho1 which binds Slpr but does not localize to the membrane, does not induce apoptosis when overexpressed (Fig. 5 C).

Cdc42 and Rac1 interactions with Slpr are strongly CRIB domain dependent (Fig. 4 C). Consistent with previous studies, Cdc42 and Rac1 bind to Slpr preferentially in the GTP-bound state (Fig. 4; for review see Gallo and Johnson, 2002). In contrast, binding of Rho1 to Slpr seems independent of the CRIB domain and is strikingly GTP independent. In addition, only Rho1 shows a strong dependence on the kinase domain for Slpr binding, suggesting that it interacts with Slpr through a fundamentally different mechanism than do the other Rho family GTPases. Further dissection of the Rho1-binding domain of Slpr may shed light on how Rho1 binding affects Slpr activity.

A remaining question is whether the ability of Rho1 and Moe to control apoptosis is developmentally regulated in epithelial tissues. Previous studies have demonstrated that Moe activation and its ability to down-regulate Rho1 activity is controlled by a Sterile-20 kinase, Slik (Hipfner et al., 2004; Hughes and Fehon, 2006; Carreno et al., 2008; Kunda et al., 2008). Additionally, Slik itself has been demonstrated to be required for cell survival (Hipfner and Cohen, 2003). However, at the moment, little is known about how Slik activity may be regulated in development. Further work will be required to understand the roles of Slik, Moe, and Rho1 in regulating apoptosis in developing tissues as well as their possible role in other nondevelopmental events such as tissue homeostasis or response to wounding, in which epithelial integrity and apoptosis function coordinately.

Materials and methods

Drosophila stocks and crosses

All crosses were performed at 25°C. *Moe* double-stranded RNA depletion experiments were performed using a *dpp^{blnk}-Gal4*, *UAS-MoeRNAi*, *UAS-GFP^{NLS}/TM6B* recombinant line. The *MoeRNAi* transgene (provided by D. Ready, Purdue University, West Lafayette, IN) was described previously (Karagiosis and Ready, 2004). All other experiments using the *dpp-Gal4* driver were performed using a *dpp^{blnk}-Gal4*, *UAS-GFP^{NLS}/TM6B* recombinant line. Half-rescued imaginal discs were generated by crossing *Moe^{G0323}/FM7-GFP* (Speck et al., 2003; Karagiosis and Ready, 2004) to *enGal4*; UAS-*Myc-Moe*. The UAS-*Rho1^{+}* 2.1A and UAS-*Rho1^{N19}* transgenes used for overexpression experiments were provided by M. Mlodzik (Mount Sinai School of Medicine, New York, NY). Genetic interaction tests between JNK signaling components in Moe-deficient or Rho1-overexpressing cells were performed using the following stocks: *UAS-Tak1RNAi* 1388R-1, *UAS-slprRNAi* 2272R-1, *UAS-hepRNAi* 4353R-2, 4353R-3, and *UAS-bskRNAi* 5680R-1 (obtained from the National Institute of Genetics stock center, Japan), *UAS-egr RNAi*, *UAS-wgn RNAi*, and *UAS-dAsk1 DN* (provided by M. Miura, University of Tokyo, Bunkyo-ku, Tokyo, Japan), *UAS-Tak1 DN* (provided by T. Adachi-Yamada, Kobe University, Kobe, Japan), *UAS-Mekk1RNAi* (provided by B. Lemaitre, École Polytechnique Fédérale de Lausanne, Lausanne, Switzerland), *UAS-POSHRNAi* (#26655-line A; #26657-line B; obtained from the Vienna Drosophila RNAi Center), and *UAS-Myc-puc* (provided by D. McEwen, University of Texas Health Science Center at San Antonio, San Antonio, TX). The *Cdc42^{4}* allele was described previously (Genova et al., 2000). A *UAS-Timp* transgene was expressed to block the activity of matrix metalloproteinases (provided by A. Page-McCaw, Rensselaer Polytechnic Institute, Troy, NY). The *Rac1^{j11} Rac2$^{\Delta}$ Mtl$^{\Delta}$/TM6B*, *Rho1$^{E3.10}$/Cyo*, *UAS-rokCAT3.1*, *UAS-bskDN*, and *UAS-LacZ* lines were obtained from the Bloomington Stock Center. Recombinant lines used were *UAS-slprRNAi, puc^{E69}/TM6B*, *UAS-hepRNAi, puc^{E69}/TM6B*, *UAS-Rho1, puc^{E69}/TM6B*, and *UAS-Rho1, hid-lacZ/TM6B*. The presence of the *lacZ* reporter in each was confirmed by β-galactosidase staining.

Immunostaining

Wandering third instar wing discs were dissected in Schneider's medium containing serum and fixed in 2% paraformaldehyde solution for 20 min. To compare Rho1 transgene expression levels, each genotype was stained using the same antibody solutions and imaged using the same confocal gain and offset settings. To observe cortical Rho1 localization, discs were fixed in 10% TCA on ice for 20 min. Antibodies were used at the following concentrations: rabbit anti–cleaved caspase-3 at 1:1,000 (Cell Signaling Technology), mouse anti-MMP1 at 1:300 (cocktail of 3A6B4, 3B68D12, 5H7B11; Developmental Studies Hybridoma Bank), rat anti–DE-cadherin (DCAD2) at 1:250 (Developmental Studies Hybridoma Bank), mouse anti-Moe at 1:40,000, rabbit anti-Moe at 1:20,000 (provided by D. Kiehart, Duke University, Durham, NC), mouse anti–β-galactosidase at 1:1,000 (Promega), mouse anti-Rho1 (P1D9) at 1:50 (Developmental Studies Hybridoma Bank), rat anti–phospho-ERM (297S) at 1:10 (provided by S. Tsukita, Kyoto University, Kyoto, Japan; Matsui et al., 1998), rabbit anti-Dia at 1:5,000 (Afshar et al., 2000), rabbit anti-Slpr at 1:400 (Polaski et al., 2006), and rabbit anti–laminin A (provided by J. Fessler, University of California, Los Angeles, Los Angeles, CA). Fluorescent secondary antibodies were obtained from Jackson ImmunoResearch Laboratories, Inc. and used at a dilution of 1:1,000. Tissues were mounted in ProLong Antifade (Invitrogen). Confocal images were taken on a laser-scanning confocal microscope (LSM510; Carl Zeiss, Inc.) using the LSM acquisition software (Carl Zeiss, Inc.) and either a 40× NA 1.3 EC Plan-NeoFluar objective or a 20× NA 0.8 Plan-Apochromat objective. Images were then compiled in Photoshop 7.0 (Adobe).

Expression constructs

cDNA clones for *Rho1*, *Rac1*, and *Cdc42* were used as templates for PCR amplification reactions using gene-specific primers that added 5′ BamHI and 3′ EcoRI restriction sites. These PCR products were then subcloned into the Gateway entry vector pENTR3C (Invitrogen). Site-directed mutagenesis using mutagenic primers was performed on the pENTR3C constructs to make the *Rho1^{V14}*, *Rho1^{N19}*, *Rho1^{C189S}*, *Rac1^{V12}*, *Rac1^{N17}*, *Cdc42^{V12}*, and *Cdc42^{N17}* constructs. LR Clonase recombination reactions were then performed to put these constructs into the pAFW (actin promoter, 3× N-terminal Flag tag), pAHW (actin promoter, 3× N-terminal HA tag), and pTW (derived from pUAST, untagged) vectors (obtained from the Drosophila Genomics Resource Center).

P-element transformation was used to generate *Rho1^{C189S}* transgenic lines (Duke University Model Systems Genomics). Multiple lines were tested and found to have similar effects. Two individual lines with different expression levels were used for further analysis.

slpr was PCR amplified from the cDNA clone GH26507 (Drosophila Genomics Resource Center) with primers incorporating a 5′ KpnI and 3′ EcoRI restriction site. This PCR fragment was then subcloned into the pENTR3C vector. Because the original EST contains a point mutation changing amino acid D314 to Y (reported in Polaski et al., 2006), site-directed mutagenesis was performed on this subclone to change the mutation back to the original amino acid. This clone was then used as the template for all further experiments. All *slpr* fragments were PCR amplified with 5′ KpnI and 3′ EcoRI restriction sites and cloned into the pENTR3C vector. The deletions of the CRIB (deletes aa 503–514) and kinase domain (deletes aa 141–445) were performed using site-directed mutagenesis. LR Clonase reactions were performed to put *slpr* constructs into the pAW (actin promoter, untagged), pAFW, and pAHW vectors.

Tak1 was PCR amplified from the cDNA clone LD42274 (Drosophila Genomics Resource Center) with primers incorporating a 5′ KpnI and 3′ XhoI restriction site. This PCR fragment was then subcloned into the pENTR3C vector. LR Clonase reactions were performed to put *Tak1* into the pAFW and pAHW vectors. The UAS-POSH-Flag construct was provided by N. Harden (Simon Fraser University, Burnaby, British Columbia, Canada).

UAS-dia RNAi construct

To build the *UAS-dia* RNAi transgene, nt 1542–2088 from dia were PCR amplified with primers incorporating a 5′ BamHI and 3′ EcoRI site using a *dia* cDNA (provided by S. Wasserman, University of California, San Diego, La Jolla, CA). This PCR product was cloned into the pENTR3C vector and then transferred into the pRISE (Kondo et al., 2006) destination vector using a LR Clonase reaction. The resulting pRISE *dia* RNAi clone was checked for proper recombination. *P*-element transformation was used to generate transgenic lines (Duke University Model Systems Genomics). To provide better knockdown of Dia protein, a recombinant line carrying two copies of the *UAS-dia* RNAi was used.

IPs

8.0×10^6 S2 cells were transfected with the indicated constructs using DDAB (dimethyldioctadecyl-ammonium bromide) at 250 µg/ml

(Sigma-Aldrich; Han, 1996), with the exception of the $Rho1^{N19}$ IP experiment to look for co-IP of endogenous Slpr, which used 1.6×10^7 S2 cells. IPs were performed 2 d after transfection. Cells were harvested and lysed in buffer containing 50 mM Hepes, 150 mM NaCl, 1 mM EDTA, 0.5 mM EGTA, 0.9 M glycerol, 0.1% Triton X-100, 0.5 mM DTT, and Complete protease inhibitor cocktail (Roche). Flag IPs were performed using anti-Flag M2 agarose beads (Sigma-Aldrich). IP reactions were performed at 4°C for 2 h. For immunoblotting, 4–20 or 5–15% gradient SDS-PAGE gels were used and transferred onto nitrocellulose. Antibodies were used at the following concentrations: mouse anti-Flag M2 at 1:20,000 (Sigma-Aldrich), rabbit anti-Slpr at 1:2,000 (affinity purified) or 1:10,000 (sera), and rabbit anti-HA at 1:5,000 (Rockland). Fluorescently labeled IRdye800 (Rockland) and Alexa Fluor 680 (Invitrogen) secondary antibodies were used at a concentration of 1:5,000. Images of the blots were obtained using Odyssey with version 2.1 software (LI-COR Biosciences).

GST pull-down assay with IVT-labeled input

DNA inserts used for in vitro transcription/translation reactions were PCR amplified using the Slpr EST GH26507 (with the D314Y polymorphism) as a template and primers encoding Nde1 restriction enzyme sites. Purified inserts were digested and ligated into the similarly digested pET-16b HIS tag vector (EMD). The construct encodes aa 14–540, including the SH3, kinase, Leu zipper, and CRIB domains. In vitro protein synthesis and labeling was performed in a rabbit reticulocyte lysate using the TNT Quick Coupled Transcription/Translation System (Promega) according to the manufacturer's instructions. 2–4 µl of the lysate from 50 µl of labeling reactions was used in each pull-down reaction.

pGEX expression plasmids for *Drosophila Rho1*, *Rac1*, and *Cdc42* were obtained from J. Settleman (Massachusetts General Hospital, Harvard Medical School, Charlestown, MA; Lu and Settleman, 1999). GST fusion proteins were induced in *Escherichia coli BL21* cells with 0.1 mM IPTG and prepared according to standard procedures for soluble protein (Rebay and Fehon, 2000). Purified GST and GST-GTPases bound to glutathione-agarose beads (50–100 µg/assay) were loaded with GDP or GTP-γS as described previously (Lu and Settleman, 1999). Nucleotide exchange was terminated with 20 mM $MgCl_2$. The beads were then incubated at 4°C with an equal bead volume of wash buffer (20 mM Hepes, pH 7.5, 150 mM NaCl, 10% glycerol, and 0.1% Triton X-100) plus the in vitro–labeled Slpr protein fragments for ~1 h. Reactions were washed five times with excess wash buffer; the beads were then boiled in 2× Laemmli sample buffer and analyzed by SDS-PAGE and autoradiography.

β-Galactosidase staining and adult wings

For β-galactosidase staining, wing imaginal discs of the indicated genotypes (Fig. S1) were dissected, fixed in 3.7% formaldehyde for 10 min, and stained using X-Gal staining solution as previously described (Hazelrigg, 2000). Adult wings were mounted in Aqua PolyMount (Polysciences, Inc.). Brightfield images were captured using a microscope (Axioplan 2ie; Carl Zeiss, Inc.) with 5× NA 0.15 or 10× NA 0.3 Plan-NeoFluar objectives and a camera (Spot RT; Diagnostic Instruments, Inc.) with the Spot Advanced software, version 4.0.2 (Diagnostic Instruments, Inc.). Images were compiled using Photoshop 7.0.

Quantification of pixel intensities

Images were processed using Photoshop 7.0 software. Quantification of pixel intensities was performed using ImageJ software (National Institutes of Health) on rectangular sections as indicated to display a column plot mean. For each given graph, the x axis represents the distance across the image (from anterior to posterior), and the y axis is the vertically averaged pixel intensity at a given point (x).

Online supplemental material

Fig. S1 shows that loss of *Moe* function induces JNK pathway activation and apoptosis. Fig. S2 shows quantification of the effects of loss and gain of *Moe* function on cortical Rho1 in the imaginal epithelium. Fig. S3 shows that Rho1 effectors Dia and Rok do not appear to be involved in Rho1-induced apoptosis. Fig. S4 shows that Rho1, Tak1, Slpr, and POSH coimmunoprecipitate in S2 cells. Fig. S5 shows that the CAAX box mutation in Rho1 ($Rho1^{C189S}$) is expressed at comparable levels with the wild-type and DN transgenes and coimmunoprecipitates with Slpr. Online supplemental material is available at http://www.jcb.org/cgi/content/full/jcb.200912010/DC1.

We thank M. Miura, B. Lemaitre, D. McEwen, T. Adachi-Yamada, A. Page-McCaw, D. Ready, M. Mlodzik, and the National Institute of Genetics, Vienna Drosophila RNAi Center, and Bloomington stock centers for providing fly stocks; J. Fessler, D. Kiehart, S. Tsukita, and the Developmental Studies Hybridoma Bank for providing antibodies; N. Harden for the Flag-tagged POSH construct; E. Ferguson, M. Glotzer, G. Marqués, I. Rebay, and P. Vanderzalm for comments and suggestions on the manuscript; and Fehon and Rebay laboratory members for suggestions throughout this work.

This work was funded by grants HD045836 (to B. Stronach) and GM087588 and NS034783 (to R.G. Fehon) from the National Institutes of Health.

Submitted: 2 December 2009
Accepted: 25 March 2010

References

Adachi-Yamada, T., and M.B. O'Connor. 2002. Morphogenetic apoptosis: a mechanism for correcting discontinuities in morphogen gradients. *Dev. Biol.* 251:74–90. doi:10.1006/dbio.2002.0821

Afshar, K., B. Stuart, and S.A. Wasserman. 2000. Functional analysis of the *Drosophila* diaphanous FH protein in early embryonic development. *Development*. 127:1887–1897.

Agnès, F., M. Suzanne, and S. Noselli. 1999. The *Drosophila* JNK pathway controls the morphogenesis of imaginal discs during metamorphosis. *Development*. 126:5453–5462.

Bangi, E., and K. Wharton. 2006. Dpp and Gbb exhibit different effective ranges in the establishment of the BMP activity gradient critical for *Drosophila* wing patterning. *Dev. Biol.* 295:178–193. doi:10.1016/j.ydbio.2006.03.021

Bloor, J.W., and D.P. Kiehart. 2002. *Drosophila* RhoA regulates the cytoskeleton and cell-cell adhesion in the developing epidermis. *Development*. 129:3173–3183.

Böck, B.C., P.O. Vacratsis, E. Qamirani, and K.A. Gallo. 2000. Cdc42-induced activation of the mixed-lineage kinase SPRK in vivo. Requirement of the Cdc42/Rac interactive binding motif and changes in phosphorylation. *J. Biol. Chem.* 275:14231–14241. doi:10.1074/jbc.275.19.14231

Bretscher, A., K. Edwards, and R.G. Fehon. 2002. ERM proteins and merlin: integrators at the cell cortex. *Nat. Rev. Mol. Cell Biol.* 3:586–599. doi:10.1038/nrm882

Brun, S., S. Vidal, P. Spellman, K. Takahashi, H. Tricoire, and B. Lemaitre. 2006. The MAPKKK Mekk1 regulates the expression of Turandot stress genes in response to septic injury in *Drosophila*. *Genes Cells*. 11:397–407. doi:10.1111/j.1365-2443.2006.00953.x

Burbelo, P.D., D. Drechsel, and A. Hall. 1995. A conserved binding motif defines numerous candidate target proteins for both Cdc42 and Rac GTPases. *J. Biol. Chem.* 270:29071–29074. doi:10.1074/jbc.270.49.29071

Carreno, S., I. Kouranti, E.S. Glusman, M.T. Fuller, A. Echard, and F. Payre. 2008. Moesin and its activating kinase Slik are required for cortical stability and microtubule organization in mitotic cells. *J. Cell Biol.* 180:739–746. doi:10.1083/jcb.200709161

Chakrabandhu, K., Z. Hérincs, S. Huault, B. Dost, L. Peng, F. Conchonaud, D. Marguet, H.T. He, and A.O. Hueber. 2007. Palmitoylation is required for efficient Fas cell death signaling. *EMBO J.* 26:209–220. doi:10.1038/sj.emboj.7601456

Chorna-Ornan, I., V. Tzarfaty, G. Ankri-Eliahoo, T. Joel-Almagor, N.E. Meyer, A. Huber, F. Payre, and B. Minke. 2005. Light-regulated interaction of Dmoesin with TRP and TRPL channels is required for maintenance of photoreceptors. *J. Cell Biol.* 171:143–152. doi:10.1083/jcb.200503014

Collins, C.A., Y.P. Wairkar, S.L. Johnson, and A. DiAntonio. 2006. Highwire restrains synaptic growth by attenuating a MAP kinase signal. *Neuron*. 51:57–69. doi:10.1016/j.neuron.2006.05.026

D'Angelo, R., S. Aresta, A. Blangy, L. Del Maestro, D. Louvard, and M. Arpin. 2007. Interaction of ezrin with the novel guanine nucleotide exchange factor PLEKHG6 promotes RhoG-dependent apical cytoskeleton rearrangements in epithelial cells. *Mol. Biol. Cell*. 18:4780–4793. doi:10.1091/mbc.E06-12-1144

Dhanasekaran, D.N., K. Kashef, C.M. Lee, H. Xu, and E.P. Reddy. 2007. Scaffold proteins of MAP-kinase modules. *Oncogene*. 26:3185–3202. doi:10.1038/sj.onc.1210411

Dovas, A., and J.R. Couchman. 2005. RhoGDI: multiple functions in the regulation of Rho family GTPase activities. *Biochem. J.* 390:1–9. doi:10.1042/BJ20050104

Gallo, K.A., and G.L. Johnson. 2002. Mixed-lineage kinase control of JNK and p38 MAPK pathways. *Nat. Rev. Mol. Cell Biol.* 3:663–672. doi:10.1038/nrm906

Gautreau, A., P. Poullet, D. Louvard, and M. Arpin. 1999. Ezrin, a plasma membrane-microfilament linker, signals cell survival through the

phosphatidylinositol 3-kinase/Akt pathway. *Proc. Natl. Acad. Sci. USA*. 96:7300–7305. doi:10.1073/pnas.96.13.7300

Genova, J.L., S. Jong, J.T. Camp, and R.G. Fehon. 2000. Functional analysis of Cdc42 in actin filament assembly, epithelial morphogenesis, and cell signaling during *Drosophila* development. *Dev. Biol.* 221:181–194. doi:10.1006/dbio.2000.9671

Geuking, P., R. Narasimamurthy, and K. Basler. 2005. A genetic screen targeting the tumor necrosis factor/Eiger signaling pathway: identification of *Drosophila* TAB2 as a functionally conserved component. *Genetics*. 171:1683–1694. doi:10.1534/genetics.105.045534

Glise, B., H. Bourbon, and S. Noselli. 1995. hemipterous encodes a novel *Drosophila* MAP kinase kinase, required for epithelial cell sheet movement. *Cell*. 83:451–461. doi:10.1016/0092-8674(95)90123-X

Göbel, V., P.L. Barrett, D.H. Hall, and J.T. Fleming. 2004. Lumen morphogenesis in *C. elegans* requires the membrane-cytoskeleton linker erm-1. *Dev. Cell*. 6:865–873. doi:10.1016/j.devcel.2004.05.018

Halsell, S.R., B.I. Chu, and D.P. Kiehart. 2000. Genetic analysis demonstrates a direct link between rho signaling and nonmuscle myosin function during *Drosophila* morphogenesis. *Genetics*. 155:1253–1265.

Han, K. 1996. An efficient DDAB-mediated transfection of *Drosophila* S2 cells. *Nucleic Acids Res.* 24:4362–4363. doi:10.1093/nar/24.21.4362

Hatzoglou, A., I. Ader, A. Splingard, J. Flanders, E. Saade, I. Leroy, S. Traver, S. Aresta, and J. de Gunzburg. 2007. Gem associates with Ezrin and acts via the Rho-GAP protein Gmip to down-regulate the Rho pathway. *Mol. Biol. Cell*. 18:1242–1252. doi:10.1091/mbc.E06-06-0510

Hazelrigg, T. 2000. GFP and other reporters. In *Drosophila* Protocols. W. Sullivan, M. Ashburner, and R.S. Hawley, editors. Cold Spring Harbor Laboratory Press, Cold Spring Harbor, NY. 313–343.

Hipfner, D.R., and S.M. Cohen. 2003. The *Drosophila* sterile-20 kinase slik controls cell proliferation and apoptosis during imaginal disc development. *PLoS Biol.* 1:E35. doi:10.1371/journal.pbio.0000035

Hipfner, D.R., N. Keller, and S.M. Cohen. 2004. Slik Sterile-20 kinase regulates Moesin activity to promote epithelial integrity during tissue growth. *Genes Dev.* 18:2243–2248. doi:10.1101/gad.303304

Holley, C.L., M.R. Olson, D.A. Colón-Ramos, and S. Kornbluth. 2002. Reaper eliminates IAP proteins through stimulated IAP degradation and generalized translational inhibition. *Nat. Cell Biol.* 4:439–444. doi:10.1038/ncb798

Hughes, S.C., and R.G. Fehon. 2006. Phosphorylation and activity of the tumor suppressor Merlin and the ERM protein Moesin are coordinately regulated by the Slik kinase. *J. Cell Biol.* 175:305–313. doi:10.1083/jcb.200608009

Igaki, T., H. Kanda, Y. Yamamoto-Goto, H. Kanuka, E. Kuranaga, T. Aigaki, and M. Miura. 2002. Eiger, a TNF superfamily ligand that triggers the *Drosophila* JNK pathway. *EMBO J.* 21:3009–3018. doi:10.1093/emboj/cdf306

Igaki, T., R.A. Pagliarini, and T. Xu. 2006. Loss of cell polarity drives tumor growth and invasion through JNK activation in *Drosophila*. *Curr. Biol.* 16:1139–1146. doi:10.1016/j.cub.2006.04.042

Janody, F., and J.E. Treisman. 2006. Actin capping protein alpha maintains vestigial-expressing cells within the *Drosophila* wing disc epithelium. *Development*. 133:3349–3357. doi:10.1242/dev.02511

Karagiosis, S.A., and D.F. Ready. 2004. Moesin contributes an essential structural role in *Drosophila* photoreceptor morphogenesis. *Development*. 131:725–732. doi:10.1242/dev.00976

Kim, G.H., E. Park, and J.K. Han. 2005. The assembly of POSH-JNK regulates *Xenopus* anterior neural development. *Dev. Biol.* 286:256–269. doi:10.1016/j.ydbio.2005.07.033

Kondo, T., S. Inagaki, K. Yasuda, and Y. Kageyama. 2006. Rapid construction of *Drosophila* RNAi transgenes using pRISE, a P-element-mediated transformation vector exploiting an in vitro recombination system. *Genes Genet. Syst.* 81:129–134. doi:10.1266/ggs.81.129

Kunda, P., A.E. Pelling, T. Liu, and B. Baum. 2008. Moesin controls cortical rigidity, cell rounding, and spindle morphogenesis during mitosis. *Curr. Biol.* 18:91–101. doi:10.1016/j.cub.2007.12.051

Kuo, W.C., K.T. Yang, S.L. Hsieh, and M.Z. Lai. 2010. Ezrin is a negative regulator of death receptor-induced apoptosis. *Oncogene*. 29:1374–1383. doi:10.1038/onc.2009.417

Kuranaga, E., and M. Miura. 2005. Genetic approaches for the identification of apoptotic components. *Med. Mol. Morphol.* 38:18–22. doi:10.1007/s00795-004-0276-x

Kuranaga, E., H. Kanuka, T. Igaki, K. Sawamoto, H. Ichijo, H. Okano, and M. Miura. 2002. Reaper-mediated inhibition of DIAP1-induced DTRAF1 degradation results in activation of JNK in *Drosophila*. *Nat. Cell Biol.* 4:705–710. doi:10.1038/ncb842

Lu, Y., and J. Settleman. 1999. The *Drosophila* Pkn protein kinase is a Rho/Rac effector target required for dorsal closure during embryogenesis. *Genes Dev.* 13:1168–1180. doi:10.1101/gad.13.9.1168

Luo, X., O. Puig, J. Hyun, D. Bohmann, and H. Jasper. 2007. Foxo and Fos regulate the decision between cell death and survival in response to UV irradiation. *EMBO J.* 26:380–390. doi:10.1038/sj.emboj.7601484

Ma, Z., D.P. Myers, R.F. Wu, F.E. Nwariaku, and L.S. Terada. 2007. $p66^{Shc}$ mediates anoikis through RhoA. *J. Cell Biol.* 179:23–31. doi:10.1083/jcb.200706097

Macías, A., N.M. Romero, F. Martín, L. Suárez, A.L. Rosa, and G. Morata. 2004. PVF1/PVR signaling and apoptosis promotes the rotation and dorsal closure of the *Drosophila* male terminalia. *Int. J. Dev. Biol.* 48:1087–1094. doi:10.1387/ijdb.041859am

Martín-Blanco, E., A. Gampel, J. Ring, K. Virdee, N. Kirov, A.M. Tolkovsky, and A. Martinez-Arias. 1998. puckered encodes a phosphatase that mediates a feedback loop regulating JNK activity during dorsal closure in *Drosophila*. *Genes Dev.* 12:557–570. doi:10.1101/gad.12.4.557

Masucci, J.D., R.J. Miltenberger, and F.M. Hoffmann. 1990. Pattern-specific expression of the *Drosophila* decapentaplegic gene in imaginal disks is regulated by 3′ cis-regulatory elements. *Genes Dev.* 4:2011–2023. doi:10.1101/gad.4.11.2011

Mathew, S.J., D. Haubert, M. Krönke, and M. Leptin. 2009. Looking beyond death: a morphogenetic role for the TNF signalling pathway. *J. Cell Sci.* 122:1939–1946. doi:10.1242/jcs.044487

Matsui, T., M. Maeda, Y. Doi, S. Yonemura, M. Amano, K. Kaibuchi, S. Tsukita, and S. Tsukita. 1998. Rho-kinase phosphorylates COOH-terminal threonines of ezrin/radixin/moesin (ERM) proteins and regulates their head-to-tail association. *J. Cell Biol.* 140:647–657. doi:10.1083/jcb.140.3.647

McEwen, D.G., and M. Peifer. 2005. Puckered, a *Drosophila* MAPK phosphatase, ensures cell viability by antagonizing JNK-induced apoptosis. *Development*. 132:3935–3946. doi:10.1242/dev.01949

Molnar, C., and J.F. de Celis. 2006. Independent roles of *Drosophila* Moesin in imaginal disc morphogenesis and hedgehog signalling. *Mech. Dev.* 123:337–351. doi:10.1016/j.mod.2006.02.001

Monni, R., L. Haddaoui, A. Naba, I. Gallais, M. Arpin, P. Mayeux, and F. Moreau-Gachelin. 2008. Ezrin is a target for oncogenic Kit mutants in murine erythroleukemia. *Blood*. 111:3163–3172. doi:10.1182/blood-2007-09-110510

Moreno, E., and K. Basler. 2004. dMyc transforms cells into super-competitors. *Cell*. 117:117–129. doi:10.1016/S0092-8674(04)00262-4

Moreno, E., M. Yan, and K. Basler. 2002. Evolution of TNF signaling mechanisms: JNK-dependent apoptosis triggered by Eiger, the *Drosophila* homolog of the TNF superfamily. *Curr. Biol.* 12:1263–1268. doi:10.1016/S0960-9822(02)00954-5

Park, J.M., H. Brady, M.G. Ruocco, H. Sun, D. Williams, S.J. Lee, T. Kato Jr., N. Richards, K. Chan, F. Mercurio, et al. 2004. Targeting of TAK1 by the NF-kappa B protein Relish regulates the JNK-mediated immune response in *Drosophila*. *Genes Dev.* 18:584–594. doi:10.1101/gad.1168104

Parlato, S., A.M. Giammarioli, M. Logozzi, F. Lozupone, P. Matarrese, F. Luciani, M. Falchi, W. Malorni, and S. Fais. 2000. CD95 (APO-1/Fas) linkage to the actin cytoskeleton through ezrin in human T lymphocytes: a novel regulatory mechanism of the CD95 apoptotic pathway. *EMBO J.* 19:5123–5134. doi:10.1093/emboj/19.19.5123

Piekny, A., M. Werner, and M. Glotzer. 2005. Cytokinesis: welcome to the Rho zone. *Trends Cell Biol.* 15:651–658. doi:10.1016/j.tcb.2005.10.006

Polaski, S., L. Whitney, B.W. Barker, and B. Stronach. 2006. Genetic analysis of slipper/mixed lineage kinase reveals requirements in multiple Jun-N-terminal kinase-dependent morphogenetic events during *Drosophila* development. *Genetics*. 174:719–733. doi:10.1534/genetics.106.056564

Rebay, I., and R. Fehon. 2000. Antibodies against *Drosophila* proteins. In *Drosophila* Protocols. W. Sullivan, M. Ashburner, and R.S. Hawley, editors. Cold Spring Harbor Laboratory Press, Cold Spring Harbor, NY. 389–411.

Ryabinina, O.P., E. Subbian, and M.S. Iordanov. 2006. D-MEKK1, the *Drosophila* orthologue of mammalian MEKK4/MTK1, and Hemipterous/D-MKK7 mediate the activation of D-JNK by cadmium and arsenite in Schneider cells. *BMC Cell Biol.* 7:7. doi:10.1186/1471-2121-7-7

Saotome, I., M. Curto, and A.I. McClatchey. 2004. Ezrin is essential for epithelial organization and villus morphogenesis in the developing intestine. *Dev. Cell*. 6:855–864. doi:10.1016/j.devcel.2004.05.007

Speck, O., S.C. Hughes, N.K. Noren, R.M. Kulikauskas, and R.G. Fehon. 2003. Moesin functions antagonistically to the Rho pathway to maintain epithelial integrity. *Nature*. 421:83–87. doi:10.1038/nature01295

Stronach, B., and N. Perrimon. 2002. Activation of the JNK pathway during dorsal closure in *Drosophila* requires the mixed lineage kinase, slipper. *Genes Dev.* 16:377–387. doi:10.1101/gad.953002

Takahashi, K., T. Sasaki, A. Mammoto, K. Takaishi, T. Kameyama, S. Tsukita, and Y. Takai. 1997. Direct interaction of the Rho GDP dissociation inhibitor with ezrin/radixin/moesin initiates the activation of the

Rho small G protein. *J. Biol. Chem.* 272:23371–23375. doi:10.1074/jbc.272.37.23371

Takahashi, K., T. Sasaki, A. Mammoto, I. Hotta, K. Takaishi, H. Imamura, K. Nakano, A. Kodama, and Y. Takai. 1998. Interaction of radixin with Rho small G protein GDP/GTP exchange protein Dbl. *Oncogene*. 16:3279–3284. doi:10.1038/sj.onc.1201874

Takatsu, Y., M. Nakamura, M. Stapleton, M.C. Danos, K. Matsumoto, M.B. O'Connor, H. Shibuya, and N. Ueno. 2000. TAK1 participates in c-Jun N-terminal kinase signaling during *Drosophila* development. *Mol. Cell. Biol.* 20:3015–3026. doi:10.1128/MCB.20.9.3015-3026.2000

Takeda, K., T. Noguchi, I. Naguro, and H. Ichijo. 2008. Apoptosis signal-regulating kinase 1 in stress and immune response. *Annu. Rev. Pharmacol. Toxicol.* 48:199–225. doi:10.1146/annurev.pharmtox.48.113006.094606

Tapon, N., K. Nagata, N. Lamarche, and A. Hall. 1998. A new rac target POSH is an SH3-containing scaffold protein involved in the JNK and NF-kappaB signalling pathways. *EMBO J.* 17:1395–1404. doi:10.1093/emboj/17.5.1395

Teramoto, H., O.A. Coso, H. Miyata, T. Igishi, T. Miki, and J.S. Gutkind. 1996. Signaling from the small GTP-binding proteins Rac1 and Cdc42 to the c-Jun N-terminal kinase/stress-activated protein kinase pathway. A role for mixed lineage kinase 3/protein-tyrosine kinase 1, a novel member of the mixed lineage kinase family. *J. Biol. Chem.* 271:27225–27228. doi:10.1074/jbc.271.8.3963

Uhlirova, M., and D. Bohmann. 2006. JNK- and Fos-regulated Mmp1 expression cooperates with Ras to induce invasive tumors in *Drosophila*. *EMBO J.* 25:5294–5304. doi:10.1038/sj.emboj.7601401

Vidal, M., D.E. Larson, and R.L. Cagan. 2006. Csk-deficient boundary cells are eliminated from normal *Drosophila* epithelia by exclusion, migration, and apoptosis. *Dev. Cell*. 10:33–44. doi:10.1016/j.devcel.2005.11.007

Winter, C.G., B. Wang, A. Ballew, A. Royou, R. Karess, J.D. Axelrod, and L. Luo. 2001. *Drosophila* Rho-associated kinase (Drok) links Frizzled-mediated planar cell polarity signaling to the actin cytoskeleton. *Cell*. 105:81–91. doi:10.1016/S0092-8674(01)00298-7

Woolner, S., A. Jacinto, and P. Martin. 2005. The small GTPase Rac plays multiple roles in epithelial sheet fusion—dynamic studies of *Drosophila* dorsal closure. *Dev. Biol.* 282:163–173. doi:10.1016/j.ydbio.2005.03.005

Xu, Z., N.V. Kukekov, and L.A. Greene. 2003. POSH acts as a scaffold for a multiprotein complex that mediates JNK activation in apoptosis. *EMBO J.* 22:252–261. doi:10.1093/emboj/cdg021

Yonemura, S., K. Hirao-Minakuchi, and Y. Nishimura. 2004. Rho localization in cells and tissues. *Exp. Cell Res.* 295:300–314. doi:10.1016/j.yexcr.2004.01.005

Yoo, S.J., J.R. Huh, I. Muro, H. Yu, L. Wang, S.L. Wang, R.M. Feldman, R.J. Clem, H.A. Müller, and B.A. Hay. 2002. Hid, Rpr and Grim negatively regulate DIAP1 levels through distinct mechanisms. *Nat. Cell Biol.* 4:416–424. doi:10.1038/ncb793